Resonant photoelectron spectroscopy on CoO

1997 J. Phys.: Condens. Matter 9 9863

(http://iopscience.iop.org/0953-8984/9/45/014)

J. Phys.: Condens. Matter **9** (1997) 9863–9871. Printed in the UK PII: S0953-8984(97)83631-4

Resonant photoelectron spectroscopy on CoO

O Tjernberg†§, G Chiaia†‖, U O Karlsson† and F M F de Groot‡

† Materials Physics, Royal Institute of Technology, S-100 44 Stockholm, Sweden

‡ Department of Applied Physics, Rijksuniversiteit Groningen, Nijenborgh 4, 9747 AG Groningen, The Netherlands

Received 23 April 1997, in final form 1 September 1997

Abstract. Resonant photoelectron spectroscopy data from *in situ* cleaved CoO single crystals are presented. Valence band data collected at photon energies corresponding to Co $2p_{3/2}$ are discussed in comparison with a cluster model calculation and quantitative estimates of the model parameters are given. No valence band resonance is observed at the O 1s absorption threshold but the similarity between the observed Auger lines and those previously observed for NiO confirm the similarity between the O valence band states in the two materials.

1. Introduction

The study of strongly correlated electronic systems in solid-state physics goes back to the beginning of the century when it was realized that some materials like the transition metal oxides CoO and NiO are insulating when a valence count indicates that they should have half-filled bands and therefore be conducting. Still today there is no general consensus on how to best describe the electronic structure of these materials. The general theory for electronic structure in use today is the density functional theory (DFT) [1–3]. In practice this theory is often applied by using the local density approximation (LDA) or its spin-resolved equivalent the LSDA. The LDA or LSDA fail, however, even to predict the correct ground state for CoO. According to LSDA band-structure calculations, CoO should be a metal when it is in fact an antiferromagnetic insulator. This failure is most probably caused by inadequate description of the correlation effects stemming from the Coulomb interactions. Mott was one of the first to describe these effects [4] which were later extended by Hubbard [5] who introduced the so-called Hubbard model. This model has been extensively studied in recent years in connection with high-temperature superconductivity [6].

In the interpretation of spectroscopic data on transition metal oxides the single-impurity model is often used. In this model, the transition metal atom is considered as a localized impurity in the ligand matrix. Within the impurity model, satellite features like the ones observed for transition metal oxides can often be given a straightforward explanation. LDA band-structure calculations fail in most cases to explain these satellites.

In determining the parameters of model Hamiltonians, photoelectron spectroscopy is often very useful, especially so resonant photoelectron spectroscopy (RPES). By comparing cluster model calculations with RPES data, numerical estimates of such parameters as the charge-transfer energy and the intra-atomic Coulomb repulsion can be made.

§ Present address: European Synchrotron Radiation Facility, BP 220, F-38043 Grenoble Cédex, France.

‖ Present address: INFM-Dipartimento di Fisica, Politecnico di Milano, Piazza L Da Vinci 32, 20133 Milano, Italy.

0953-8984/97/459863+09$19.50

In this report such a comparison is made between valence band data for CoO and a cluster model calculation which includes the effects of the two-electron integrals (multiplets), the crystal field and charge transfer.

2. Experimental procedure

The data were collected at beam line 22 [7] at Max-lab, the Swedish national synchrotron radiation facility. This beam-line is equipped with a modified SX-700 planar grating monochromator and a 200 mm mean radius hemispherical analyser with a multichannel detector. The set-up enabled energy resolutions of 0.6 eV and 0.4 eV to be achieved at the Co 2p and O 1s absorption edges respectively. The sample was cleaved *in situ* at a base pressure of $\sim 2 \times 10^{-10}$ Torr. After cleavage, the surface quality was checked by low-energy electron diffraction (LEED) showing sharp 1×1 spots and then transferred into the measurement chamber. The base pressure in the measurement chamber was in the 10^{-11} torr range. Due to the insulating nature of CoO, charging effects occurred. In order to improve the conductivity the sample was heated by a resistive coil mounted behind the sample holder and the temperature verified with the aid of a thermocouple mounted on the side of the sample holder. The sample was heated to 90 °C. At this point, reduction of the photon flux had no further effect on the charging, indicating that the sample had sufficient conductivity. The sample was then kept at this temperature throughout the measurements and low-photon-energy (PE) spectra of the valence band were recorded at regular intervals to verify that no surface degradation was taking place. Calibration of the spectra was performed by measuring the gold 4f spectrum of a gold foil mounted on the sample holder.

3. The theoretical model

The calculation of the Co 3d resonant photoemission spectra was performed within a cluster model including multiplets of the localized state, the crystal field and the charge transfer. The system under consideration is a CoO_6^{10-} octahedron and the Hamiltonian used to describe this cluster can be written as: $H = H_{\text{ligand}} + H_M + H_{\text{mix}}$ where

$$H_{\text{ligand}} = \sum_{\nu} \varepsilon_l a_\nu^\dagger a_\nu$$

$$\begin{aligned} H_M = {} & \sum_{\nu} \varepsilon_d d_\nu^\dagger d_\nu + \sum_{\nu} \varepsilon_{2p} p_\nu^\dagger p_\nu + \sum_{\nu_1,\nu_2,\nu_3,\nu_4} g_{pd}(\nu_1,\nu_2,\nu_3,\nu_4) d_{\nu_1}^\dagger d_{\nu_2} p_{\nu_3}^\dagger p_{\nu_4} \\ & + \frac{1}{2} \sum_{\nu_1,\nu_2,\nu_3,\nu_4} g_{dd}(\nu_1,\nu_2,\nu_3,\nu_4) d_{\nu_1}^\dagger d_{\nu_2} d_{\nu_3}^\dagger d_{\nu_4} + D \sum_{\nu_1,\nu_2} d_{\nu_1}^\dagger d_{\nu_2} \\ & + \zeta_d \sum_{\nu_1,\nu_2} (\boldsymbol{l}\cdot\boldsymbol{s})_{\nu_1,\nu_2} d_{\nu_1}^\dagger d_{\nu_2} + \zeta_p \sum_{\nu_1,\nu_2} (\boldsymbol{l}\cdot\boldsymbol{s})_{\nu_1,\nu_2} p_{\nu_1}^\dagger p_{\nu_2} \end{aligned}$$

$$H_{\text{mix}} = \sum_{\nu} V(\nu)(d_\nu^\dagger a_\nu + a_\nu^\dagger d_\nu).$$

The Hamiltonian is written in the language of second quantization where the a-, p- and d-operators create holes in the O 2p, Co 2p and 3d orbitals respectively, and their Hermitian conjugates $a^\dagger$, $p^\dagger$ and $d^\dagger$ create electrons. ν runs over all symmetry-allowed spin orbitals. In the case of Co d levels in octahedral symmetry the irreducible representations are E_g and T_{2g} with the bases e_g and t_{2g}. The relevant Slater integrals are contained in g_{pd} and g_{dd}, and the spin–orbit parameters are denoted by ζ. H_{mix} describes the interaction between the O 2p and Co 3d states with hybridization strength $V(\nu)$. The difference between the

hybridization strengths of the e_g and t_{2g} states is taken into account by the use of the empirical relationship $V(e_g) = 2V(t_{2g})$ [8]. The H_{ligand}-part of the Hamiltonian signifies the energy of the O states and the H_M-part signifies the energy of the Co 2p and 3d states. Included in the H_M-term is also the crystal field of strength D.

The correlation energy $U_{dd} = E(d^8) + E(d^6) - 2E(d^7)$ between the 3d electrons as well as the core-hole 3d interaction Q can be defined in terms of the Slater integrals [9] but were here taken as adjustable parameters. Q was however set equal to U_{dd} in view of the experimental results as discussed below. The charge-transfer energy Δ is defined as $\Delta = E(d^8\underline{L}) - E(d^7)$ ($\underline{L}$ denotes a hole in a ligand orbital). Both the definitions of U_{dd} and Δ are taken in the limit of $V(\nu) \to 0$ and $E(d^n\underline{L}^m)$ signifies the average energy of the corresponding multiplets.

Due to the size of the Hamiltonian matrix, only d^7 and $d^8\underline{L}$ configurations were included in the calculation. This does not influence the result to any great extent since it has been shown that the $d^9\underline{L}^2$ configuration accounts for less than 1% of the ground state [10]. The wavefunctions for the initial, intermediate and final states can thus be written as $|i\rangle, |m\rangle and\ |f\rangle$ with

$$|i\rangle = \alpha_0|3d^7\rangle + \alpha_1|3d^8\underline{L}\rangle$$
$$|m\rangle = \beta_0|2p^5 3d^8\rangle + \beta_1|2p^5 3d^9\underline{L}\rangle$$
$$|f\rangle = (\gamma_0|3d^6\rangle + \gamma_1|3d^7\underline{L}\rangle) \otimes |\varepsilon\rangle$$

where $|\varepsilon\rangle$ signifies the photoelectron of energy ε. Using these wavefunctions, the photoemission spectrum as a function of the binding energy (BE) can be written as

$$I_{RPES}(E_B) = \left| \sum_{f,\nu_1,\nu_2} \langle f|\mathcal{R}_{\nu_1,\nu_2} + \mathcal{D}_{\nu_2}|i\rangle \right|^2 \delta(E_f - E_i - E_B)$$

where $\mathcal{D}_{\nu_2}$ is the direct photoemission operator giving a final state with a hole in state ν_2, and $\mathcal{R}_{\nu_1,\nu_2}$ is the resonant operator leading to the same final state as $\mathcal{D}$ but with an intermediate state characterized by a 2p core hole and an extra 3d electron ($d^\dagger_{\nu_1}$). The strength of the resonant operator $\mathcal{R}$ is approximately twenty times that of $\mathcal{D}$ for CoO at the 2p threshold. The indices run over all symmetry-allowed states.

In the calculation of the multiplet spectrum, the Slater integrals were reduced to 80% of their Hartree–Fock values as determined by atomic spectroscopy.

4. Results and discussion

In figures 1(a)–1(c), valence band spectra of CoO are displayed. The PEs used for recording the spectra are indicated on the right. The inset in figure 1(a) is the Co $2p_{3/2}$ x-ray absorption spectrum (XAS). There are three distinct features in the XAS which can be well described by multiplets in the $2p^5 3d^8$ final state [11]. Points in the XAS marked with full triangles correspond to spectra displayed in figures 1(a)–1(c). The first panel, figure 1(a), shows the spectra up to the first XAS peak. It is seen that a strong enhancement of the valence band intensity occurs at and above the absorption threshold. This is similar to what has been observed for NiO [12] and CuO [13]. The fact that the features which are enhanced remain at constant binding energy over the 2.3 eV PE region indicates that this is a resonance with a one-hole final-state and not a two-hole final-state Auger process.

As mentioned previously, the direct photoemission channel at the Co 2p absorption edge has such a low amplitude that the majority of the photoemission intensity comes from the channel involving a core hole. This makes any Fano interference effects [14] too small to

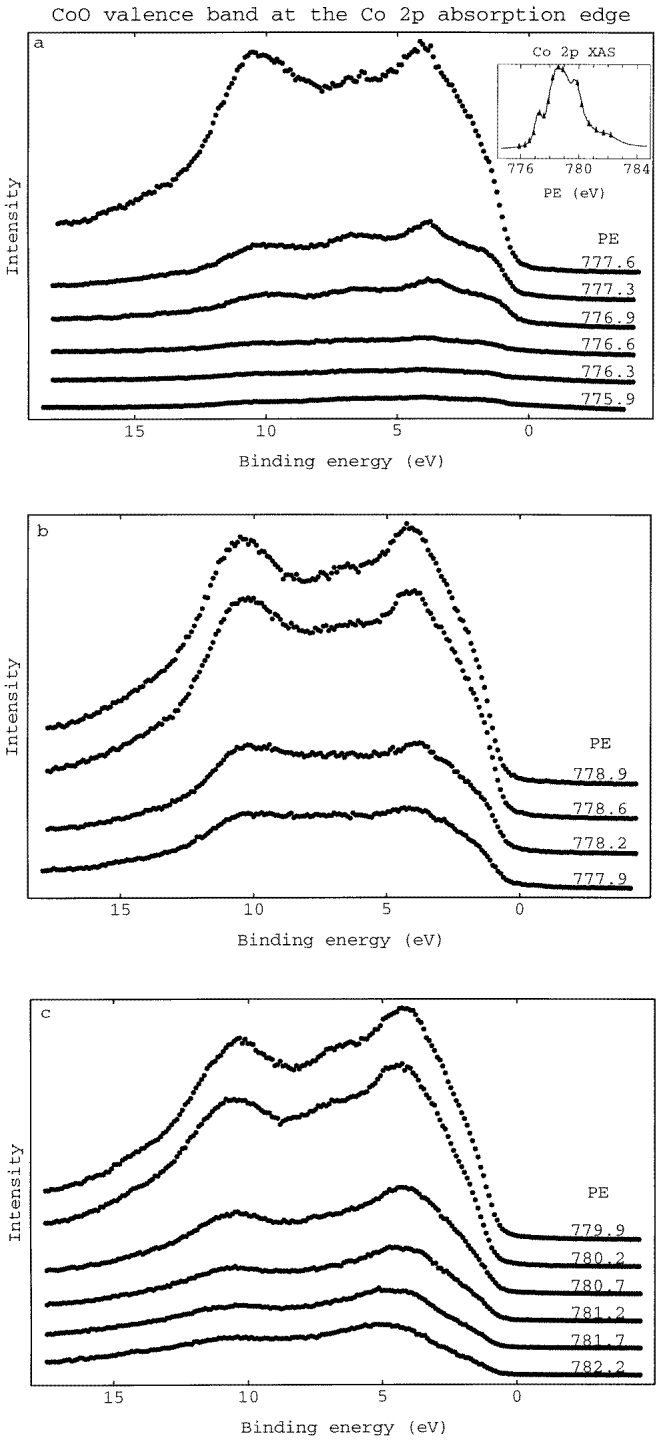

Figure 1. The CoO valence band at photon energies corresponding to the Co $2p_{3/2}$ absorption edge. The inset in (a) is the Co $2p_{3/2}$ x-ray absorption spectrum.

be visible. Four peaks located at 1.3, 3.7, 6.5 and 10.5 eV binding energy (BE) are clearly resonating. Figure 1(b), which corresponds to the main absorption peak, displays a similar behaviour. The same features are seen as in figure 1(a) and at the same positions. The 6.5 eV peak is, however, less distinct. Figure 1(c) still displays the same features as figures 1(a) and 1(b) but with an increase in the intensity of the 3.7 eV peak. Starting at a PE of approximately 781 eV, the 3.7 eV peak starts to move towards higher BE energy, indicating a transition to a two-hole Auger de-excitation. It should also be noted that the valence band intensity at the absorption edge does not follow the XAS intensity exactly, indicating that processes other than the RPES process are present [10].

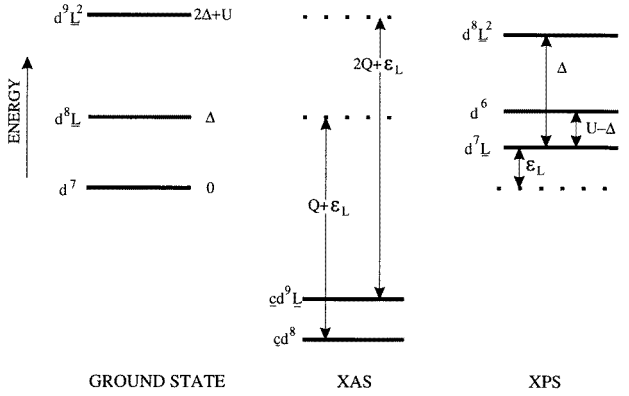

Figure 2. An energy level diagram showing the ground, XAS and final states as well as the parameters involved.

The XAS shows no satellite feature connected to a final state of mainly $2p^5 3d^9\underline{L}$ character. From the series of valence band spectra it is also clear that the resonating features stay the same throughout the PE range indicating that there is no resonance connected to a charge-transfer intermediate state (an XAS final state). In figure 2, an energy level diagram for the ground, XAS and final states is shown. The difference in energy between the $2p^5 3d^8$ and $2p^5 3d^9\underline{L}$ states is

$$\Delta + U_{dd} + Q + \epsilon_L - (2Q + \epsilon_L) = \Delta + U_{dd} - Q$$

as seen from the figure. If the ordering and spacing of the energy levels are the same in the ground and intermediate states, no satellite will be seen in the XAS and thus no satellite-related resonance will be seen in the valence band. Because no satellite structure is visible, the core-hole–d-electron interaction Q is set equal to the d–d interaction U_{dd} [15] even if a small difference is possible since Δ is quite large in the present case.

Table 1. Parameters used to calculate the spectrum displayed in figure 3 and the resulting weight of the 3d configurations.

				Weight	
Δ	U_{dd}	$V(E_g)$	$10Dq$	d^7	$d^8\underline{L}$
5.5	6.0	2.5	0.2	0.85	0.15

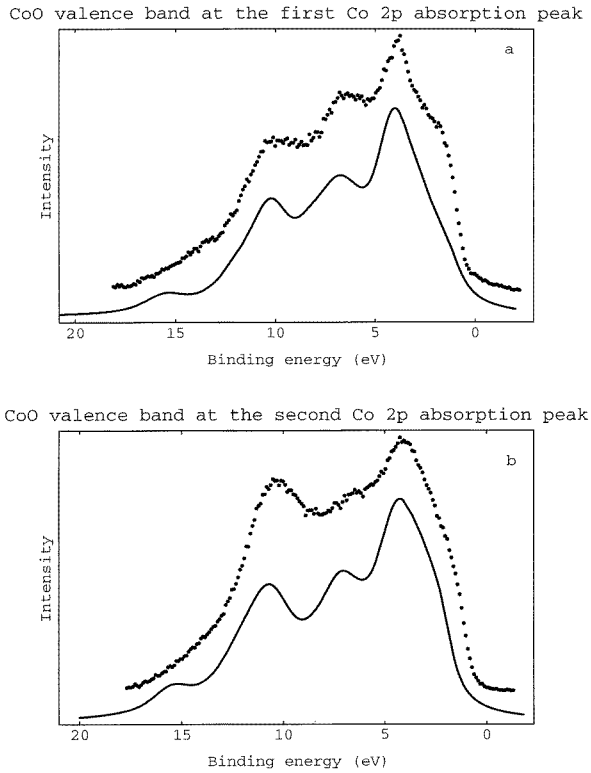

Figure 3. Comparison between calculated and measured spectra for photon energies of 777.3 and 778.9 eV

In figure 3, the result of the model calculation is displayed together with the corresponding experimental spectra. The PEs in figures 3(a) and 3(b) are that of the first and second peak in the Co $2p_{3/2}$ XAS, 777.3 eV and 778.9 eV respectively. It is seen that the experimental features are well reproduced by the calculation. The three main features show approximately the right energy spacing and relative intensity ratio, and the increase in intensity of the 10 eV BE feature between figure 3(a) and figure 3(b) is partly reproduced by the calculation. The low-BE part of the spectrum in figure 3(b) is nicely reproduced, but it seems that too much of the spectral intensity at the valence band edge in the calculated spectrum in figure 3(a) has been transferred to the 4 eV BE peak. The satellite at approximately 15 eV BE in the calculated spectra seem exaggerated as compared to the experimental spectrum. This may be partly due to background and broadening effects other than those simulated by the E^2 Lorentzian broadening applied to the calculated spectrum [16]. In order to take into account the effects of instrumental resolution, the calculated spectrum was also convoluted with a 0.5 eV full width at half-maximum (FWHM) Gaussian. The parameters adopted in the calculation are presented in table 1. It is seen that Δ is almost of the same magnitude as U_{dd}. This is not surprising in view of the following. Since the resonating states are of mainly d^6 final-state character, their position is approximately determined by $\Delta - U_{dd}$ for $\Delta > U_{dd}$ as seen from figure 2. A $\Delta \gg U_{dd}$ would place the main intensity at the valence band edge, whereas $\Delta \ll U_{dd}$ would place it far from the valence band edge. The calculated spectra are as a matter of fact more sensitive to the

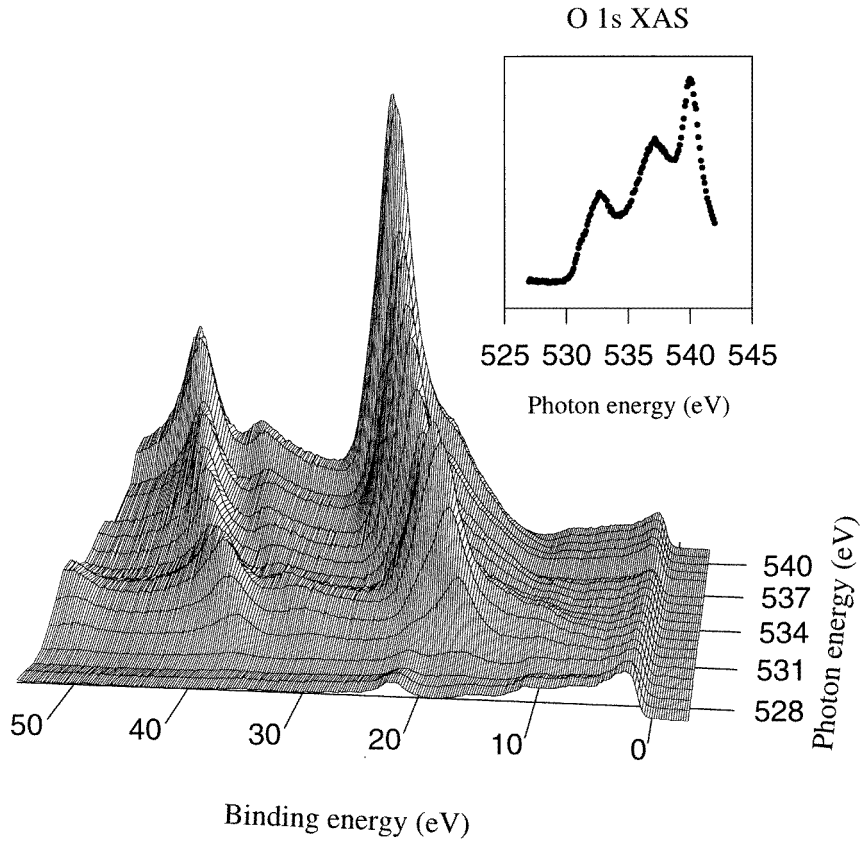

Figure 4. A mesh plot of the CoO valence band as a function of the photon energy. The inset shows the O 1s absorption spectrum.

difference $\Delta - U_{dd}$ than to the absolute values. As seen in the experimental spectra, CoO is in the intermediate regime with $\Delta \approx U_{dd}$. The Δ found here is the same as that found by van Elp [17] but one eV lower than that found by Tanaka and Jo [10]. A comparison with reference [10] shows that Tanaka and Jo's calculated spectra reproduce the experimental data presented here to a lesser extent. Kotani and Okada [18] found $\Delta = 2.5$ eV and $U_{dd} = 7.0$ eV, but these values were deduced from Co 2p photoemission which is sensitive to 2p–3d interaction and not very sensitive to the value of Δ [10]. The value of U_{dd} found here is in between those of van Elp [17] (5.4 eV) and Tanaka and Jo [10] (6.5 eV). The fact that Δ is close to but slightly lower than U_{dd} puts CoO close to the phase boundary but still in the charge-transfer region of the Zaanen–Sawatzky–Allen phase diagram [19]. It is also worth mentioning that the low $10Dq$-value of 0.2 eV is due to the fact that here the ligand field does not have to account for the charge transfer, since this is explicitly included.

Figure 4 displays spectra of the valence band recorded at PEs corresponding to the O 1s absorption edge. In figure 4 it is seen that the low-BE part of the valence band exhibits no enhancement in connection to the edge. A detailed analysis of the high-BE part of the valence band also shows that the apparent enhancement at ∼532 eV PE is only due to the low-BE tail of the strong feature seen at ∼20 eV BE. In addition to the above-mentioned strong peak at ∼20 eV BE, there is also a strong peak at ∼40 eV BE. Below the threshold, the O 2s level can be seen at approximately 22 eV BE. It is clearly seen that the two features originating at 20 and 40 eV BE follow a constant-kinetic-energy line as the PE increases. The intensities of the two peaks follow closely that of the XAS inset as expected of an Auger emission. The high- and low-BE features can be ascribed to O $KL_1L_{2,3}$ and $KL_{2,3}L_{2,3}$ Auger transitions respectively.

The BE position of the O $KL_{2,3}L_{2,3}$ transition is ∼17 eV at the absorption onset and the band gap of CoO is ∼3 eV. Using these values one finds that the main density of O states is located at 7 eV BE in agreement with earlier results [20]. This indicates that no large correlation energy is present and that the two holes resulting from the O $KL_{2,3}L_{2,3}$ Auger transition can be regarded as approximately independent. This is further supported by angle-resolved photoemission data on CoO. If the two holes resulting from an XVV Auger transition are approximately independent, then the resulting Auger spectrum can be thought of as a self-convolution of a spectrum of the valence band states involved [21]. It is therefore interesting to note that the O $KL_{2,3}L_{2,3}$ spectrum seen here closely resembles the corresponding spectrum for NiO [12]. This indicates that the O states in the valence band of NiO and CoO are very similar, confirming the similarity seen in the band-structure calculations done on these materials [20, 22].

5. Summary

It has been shown that the CoO valence band displays a very strong photoemission resonance when the photon energy is tuned to the Co $2p_{3/2}$ absorption threshold. The resonating states are of mainly d^6 final-state character, and no resonance connected to states of mainly $d^7\underline{L}$ is observed. The resonance can be well described by a cluster model calculation including multiplets and the crystal field, and the comparison between the two gives numerical estimates for the parameters of the model. In the case of CoO the charge-transfer energy Δ is found to be of almost the same magnitude as the intra-atomic Coloumb repulsion U_{dd}.

No valence band enhancements are seen at the O 1s threshold, but strong O $KL_1L_{2,3}$ and $KL_{2,3}L_{2,3}$ Auger lines are observed. The strong resemblance between the O $KL_{2,3}L_{2,3}$ line in CoO and NiO confirms that the O states in the respective valence bands are similar in nature.

References

[1] Hohenberg P and Kohn W 1964 *Phys. Rev.* **136** 3864
[2] Kohn W and Sham L J 1965 *Phys. Rev.* **140** A1133
[3] Sham L J and Kohn W 1966 *Phys. Rev.* **145** 561
[4] Mott N F 1949 *Proc. Phys. Soc.* A **62** 416
[5] Hubbard J 1963 *Proc. R. Soc.* A **276** 238
[6] Dagotto E 1994 *Rev. Mod. Phys.* **66** 763
[7] Andersen J N, Björneholm O, Sandell A, Nyholm R, Forsell J, Thånell L, Nilsson A and Mårtensson N 1991 *Synchrotr. Radiat. News* **4** (4) 15
[8] Mattheis L F 1972 *Phys. Rev.* B **5** 290
[9] Okada K and Kotani A 1992 *J. Phys. Soc. Japan* **61** 4619

[10] Tanaka A and Jo T 1994 *J. Phys. Soc. Japan* **63** 2788 and references therein
[11] de Groot F M F, Abbate M, van Elp J, Sawatzky G A, Ma Y J, Chen C T and Sette F 1993 *J. Phys.: Condens. Matter* **5** 2277
[12] Tjernberg O, Söderholm S, Karlsson U O, Chiaia G, Qvarford M, Nylén H and Lindau I 1996 *Phys. Rev.* B **53** 10 372
[13] Tjeng L H, Chen C T, Ghijsen J, Rudolf P and Sette F 1991 *Phys. Rev. Lett.* **67** 501
[14] Fano U 1961 *Phys. Rev.* **124** 1866
[15] van der Laan G, Zaanen J, Sawatzky G A, Karnatak R and Esteva J-M 1986 *Phys. Rev.* B **33** 4253
[16] The lifetime broadening of the valence band final states is mainly due to Auger decay which is approximately proportional to the square of the binding energy.
[17] van Elp J 1991 *PhD Thesis* The University of Groningen
[18] Kotani A and Okada K 1993 *Recent Advances in Magnetism of Transition Metal Compounds* ed A Kotani and N Suzuki (Singapore: World Scientific)
[19] Zaanen J, Sawatzky G A and Allen J W 1985 *Phys. Rev. Lett.* **55** 418
[20] Shen Z-X *et al* 1990 *Phys. Rev.* B **42** 1817
[21] Sawatzky G A 1989 *Auger Spectroscopy and Electronic Structure (Springer Series in Surface Science 18)* (Berlin: Springer)
[22] Shen Z-X *et al* 1991 *Phys. Rev.* B **44** 3604